CrystEngComm

Accepted Manuscript

ROYAL SOCIETY OF CHEMISTRY

www.rsc.org/crystengcomm

Growth, linear and nonlinear optical properties of DSSS crystal

Jerald V. Ramaclus*[a], Tina Thomas[b], S. Ramesh[c], P. Sagayaraj[b] and E. A. Michael[a]

[a] *Department of Electrical Engineering, University of Chile, Santiago, Chile –8370451. Email: jeraldramaclus@raig.uchile.cl, jeraldramaclus@gmail.com.*

[b] *Department of Physics, Loyola College, Chennai, India - 600034.*

[c] *Saveetha school of engineering, Saveetha University, Thandalam, Chennai, 605012, India.*

N, N-dimethylamino-N'-methylstilbazolium p-styrenesulphonate (DSSS), a stilbazolium derivative is synthesized by employing the modified counter anion approach. The growth mechanism of DSSS in methanol-water solvent system is investigated by using isothermal evaporation method and defects reveal that layered growth mechanism is adopted by DSSS. The morphology control of the crystal based on supersaturation is further investigated. Powder XRD analysis confirms that DSSS crystallizes in monoclinic system with Cc space group. The diffuse reflectance spectrum vindicates that DSSS is optically similar to N,N-dimethylamino-N'-methylstilbazolium p-toluenesulphonate (DAST). Important optical properties like absorption coefficient, refractive index and dielectric constant are reported. Second harmonic generation is found to be similar to that of DAST.

Introduction

Terahertz (THz) waves are located between microwaves and infrared light, which contain molecular information such as phonon modes of crystals, and combined modes of low frequency vibrations with rotation and tunnelling in fluids[1]. THz technology offers diverse applications such as wireless communications, inspection of drugs, detection of explosives and metals, analysis of DNA, gas sensing, imaging and spectroscopy [1-5]. The primary obstacle to realize these applications is the unavailability of terahertz sources with sufficient power, low cost, room temperature operation, frequency agility, and spectral clarity. Unfortunately, notable breakthrough has not happened with terahertz sources. However, recent developments on many aspects, like new materials, device technologies and software tools promises THz sources that can meet these requirements and the realization of these applications may not be in a very distant but near future [6,7].

Organic non-centrosymmetric, nonlinear optical (NLO) crystals are regarded as highly efficient THz emitters due to their very large NLO properties when compared to semiconductors and inorganic materials[8]. The phase velocity mismatch between the interacting waves arises due to difference in refractive indices at different wavelengths of the materials and this significantly affects the efficiency of the generated THz waves. The requirements for phase matching like birefringence, coherence length and dispersion characteristics are easily achievable in organic materials owing to their relatively low dielectric constants and large anisotropy with respect to their inorganic counterparts [9]. In addition, ionic organic crystals have their advantage of customizing the design of the molecule according to the desired properties [10]. But until now, only a few of organic materials could be crystallized in bulk size to match the requirements for device fabrication. Though DAST crystal is considered to be one of the best organic THz emitter studied so far, its growth with reasonable size coupled with high optical grade is a difficult and challenging process[11, 12].

In DAST single crystal THz waves up to 200 THz has been demonstrated by difference frequency generation (DFG) and sub-10 THz waves are also generated by optical rectification (OR) with appropriate laser setup[13,9]. However, absorption features especially at 1.1 THz in the THz spectra of DAST limits its application, and this also creates a gap in the emitted spectrum. One of the proven approaches to overcome this limitation is to modify the chemical composition of the material in order to reduce the absorption which would result in a spectrum without a gap [14]. The composition of the material is modified by changing the anion in the DAST molecule which also allows optimizing the crystal packing and orienting the dipoles as parallel as possible to develop enhanced NLO ionic organic crystal with noncentrosymmetric crystal structure[9]. In this context, a number of stilbazolium derivatives with different types of counter anions have been synthesized and investigated to understand the influence of counter anions on the growth, NLO and THz properties[15- 18]. However, the problem of phonon absorption at 1.1 THz is yet to be solved and search for an alternative is still in progress.

This article deals with N, N-dimethylamino-N'-methylstilbazolium p-styrenesulphonate (DSSS) which is made up of a positively charged nonlinear optical chromophore stilbazolium and a negatively charged anion of p-styrenesulfonate (Fig. 1). Our research group has made significant improvement in the growth characteristics of DSSS by producing crystals of size up to 3 x 2 mm^2 by successfully employing slope nucleation method coupled with slow evaporation in water-methanol solvent system (SNM-SE) when compared to other methods [18, 19]. One of the advantages of DSSS is that it grows into a noncentrosymmetric structure even in the presence of water unlike DAST and N,N-dimethylamino-N'-methylstilbazolium 2,4,6-trimethylbenzenesulphonate (DSTMS) which tend to form a hydrated centrosymmetric structure in such a case or even in methanol[13,20]. Another interesting feature of DSSS is its natural habit; it is found to have a different morphology when compared to DAST and its derivatives whose natural habit is to grow as a plates. This suggests that modification of morphology of DSSS would have different consequence and it is therefore worth investigating. Hence as a continuation, the present article aims at investigating the growth dynamics of DSSS under various supersaturations in order to maximize the size and quality of the crystal. The growth features, defects, the linear and nonlinear optical properties of the DSSS crystal are reported.

Experimental

Synthetic procedure

DSSS was synthesized according to earlier literature by performing metathesization reaction between N,N-dimethylamino-N'-methylstilbazolium iodide (DASI) salt and sodium 4-styrenesulfonate[19]. As a result of metathesization, a green precipitate was obtained which was separated from aqueous sodium iodide by vacuum filtration. The product was recrystallized from methanol several times for increasing purity of DSSS.

Crystal Growth

The previous work revealed that DSSS crystals of reasonable size could be grown from a mixed solvent system of water and methanol using SNM-SE method[19]. In the present work growth of DSSS was carried out using isothermal solvent evaporation (ISE) method in a petri dish at three different supersaturations. The first solution was prepared with 1 g of DSSS dissolved in 200 ml of methanol-water solvent system (100 ml of methanol and 100 ml of water). The dish was sealed with a perforated cap and kept in a constant temperature bath (CTB) at 35 ^{o}C. After 10 days, crystals with size up to 2 x 2 x 1 mm^3 were harvested (Fig. 2a). The second solution was prepared with 0.6 g of DSSS in a different petri dish, sealed with perforated cap and kept in the same CTB. In this case, crystals of size up to 2 x 1 x 1 mm^3 were obtained (Fig. 2b) after 10 days. The third solution was prepared by dissolving 0.01 g of DSSS in 10 ml of methanol-water solvent system at 30^{O}C. After 3 days needle like crystals of size up to 3.5 x 0.1 x 0.1 mm^3 were harvested (Fig. 2c). All the crystals, like DAST, appeared reddish upon transmission and greenish upon reflection (Fig. 2d and 2e).

Characterization

The crystallographic structure of DSSS was determined by powder X-ray diffraction analysis using a Siemens P4 Diffractometer. The surface morphology of the DSSS crystal was studied by optical microscope using Olympus-BX41-LED. Optical absorption and diffuse reflectance spectra of DSSS were measured using a Cary 5E high resolution spectrophotometer. NLO study was performed using a Q-switched Nd:YAG laser (1064nm, 10 ns pulse width and 0.68 J power, Quanta ray series, Spectra Physics). The sample was ground into very fine powder (from 50 to 100 microns) and tightly packed in a microcapillary tube. Urea crystal was taken as the reference material for comparison. The sample was then mounted in the path of the laser beam. The generated SHG signal at 532 nm is split from the fundamental frequency using an IR separator. A detector connected to a power meter is used to detect second harmonic intensity and read the energy input and output. The dielectric constant and dielectric loss of the DSSS sample were measured at different temperatures using HIOKI 3532-50 LCR HITESTER in the frequency range 100 Hz to 1 MHz. DSSS sample of uniform cross sectional area 2 x 2 mm^2 and thickness 1 mm was coated with silver paint to provide good ohmic contact. The external morphology and possible crystal growth faces of the DSSS has been predicted from its crystal structure by Bravais Friedel Donnay Harker (BFDH) method using Morphology module in the Materials studio software. The Refractive index of the DSSS crystal is calculated in the Accelrys package with CASTEP code19, which is based on density functional theory (DFT) in the local density approximation (LDA) form. The cut-off energy for the plane wave basis was set to be 400 eV and k point mesh as (4×4x1).

Results and discussion

X-ray diffraction

The powder XRD pattern of DSSS was indexed and is presented in Figure 3. The data was refined and the cell parameters were found to be a = 10.4603, b = 12.1445, c = 18.0273, α, β = 90.00 and γ = 93.39, which is in close agreement with the reported value[17]. It is observed that the crystal system, space group and cell parameters of DSSS are almost similar to that of DAST[21]. Figures 3a and 3b represent the XRD pattern of DSSS crystals grown in high supersaturation and low supersaturation respectively and Figure 3 c is that of as-synthesized DSSS powder. It is observed from the diffraction pattern (Fig. 3a) of DSSS in high supersaturation that the crystal grows as c plates with 001 as the major face; the growth rate along the c axis is the slowest when compared to a and b axes. In contrast, the low supersaturation has produced crystals with 111 (Fig. 3b) as the major face with a different morphology altogether indicating that the growth rate of faces has changed considerably when compared to the previous case. The simulated morphology of the DSSS crystal (Fig. 4) is not in exact coincidence with the morphology of the grown crystal due to the fact that solvent effect is not included. However, it can be used to identify the probable faces for consideration in comparison with the diffraction pattern.

Crystal growth dynamics and Morphology

It is observed that crystals grown from high supersaturation are parallelogram-like in shape (Fig. 2a) with large surface area and the ratio of width to surface area being at 0.25. Upon closely examining, under a microscope, the primary defect observed that is prevalent in the high supersaturation is consisting of incomplete steps (fig. 5a) which could be due to depletion of solute at the end of the growth period. The step growth or layered growth mechanism adopted by DSSS at high supersaturation is due to 2D nucleation and from the image of a completely grown crystal as shown in Figure 5b the layer formation is visible on the top side of the crystal. Those in medium supersaturation appear to be very irregular square plates stacked one over each other. Even though they are not single crystals the defects observed in these crystals reveal the growth mechanism adopted by DSSS crystals. It is

observed that the crystal´s tendency to grow into a narrow cuboid is affected, and instead of a single crystal there are either regular parallelograms (Fig. 5c) or square plates (Fig. 5d, 5e) stacked one above each other with an edge dislocation. The areas of these plates are also smaller when compared to those of high supersaturaion. At lower supersaturation the crystals appear to be perfect single crystals like long cuboids (Fig. 5f) with the ratio of width to surface area of the tip of 350 which is very high when compared to the crystals at high supersaturation.

It is known that, the growth rates of various faces are influenced by supersaturation which consequently changes the external morphology of the grown crystal[22]. It could be inferred from the micrographs that, initially, DSSS grows along the a-b axes making (001) as the major surface. However, it does not proceed in the same manner but terminates at a specific threshold governed by the supersaturation. After this it grows layers over the 001 face and this cycle repeats. When the area is large, it takes much time and solute to cover an entire layer and therefore when the growth is terminated crystals at higher supersaturation are found to have a larger (001) face than other faces. It could be observed that the surface area (001 face) is directly proportional to the supersaturation; higher the supersaturation, larger the surface area and vice versa (Fig. 6). Therefore, in lower supersaturation, the area of (001) face is small enough that the layers on top it can grow easily leading to a single crystal with (111) as the major face.

It is clear from the above defects observed that 2D nucleation is the major growth mechanism adopted by DSSS[23]. It is known that in case of DAST crystal that change in the supersaturation changes the thickness of the crystal[21]. Since DSSS is a derivative of DAST, it is expected to exhibit similar growth features and it is evident that supersaturation change along with growth method has significantly altered the morphology. The growth rate influences the size, morphology and quality of a crystal and it depends on the supersaturation. Further, it has also been reported that, by reducing the growth rate, thicker crystals are produced and the growth rate can be controlled by various parameters including temperature and supersaturation[24].

It is to be noted that the ability of DSSS to grow layers is very high when compared to DAST and other derivatives. The ratio of width to surface area is much lower in DAST than in DSSS even at higher supersaturation[19]. In the present work, it is evident that the reduced supersaturation at lower saturation temperature decreases the growth rate of surrounding faces and allows the tip to grow rapidly which changes the morphology and quality of the crystal[25]. The long needle like crystals could serve as seeds for growing large single crystals. These types of elongated crystals are attractive due to their self-waveguiding effect[26].

Linear Optical Properties

The diffuse reflectance spectrum of DSSS is shown in Figure 7a. Since the DSSS crystal is iso-structural to DAST one may not expect much deviation in the optical absorption property. Diffuse reflectance spectrum reveals three absorption bands in the infrared region at about 1200, 1400, and 1700 nm correspond to overtones of the C–H stretching vibrations and have also been observed in DAST. It has been reported that DAST crystals with a low material absorption at wavelengths of 1300 and 1550 nm are well suited for applications in telecommunications[9]. Therefore, the absorption coefficient (Fig. 7b) is calculated based on modified Kubelka-Munk equation $[a = (1 + R_\infty)^2/4R_\infty]$ for powder samples with a correction factor of 2, where R_∞ is the reflectance at a given wavelength[27]. It is assumed that the scattering coefficient is constant at all wavelengths. It is found that the absorption coefficient at important telecommunication wavelengths like 1.3 and 1.5 μm is almost around 3 cm^{-1} and when compared to DAST and DSTMS crystals the absorption coefficient is 2 times larger[13, 14]. The simulated refractive index (Fig. 7c) between 600 to 2000 nm is along x axis (n_1) is 2.2 ± 0.01 which is identical to that of DAST. The refractive index along z axis (n_3) is below 1.4 ± 0.01 which is lower than that of DAST. Therefore DSSS is strongly anisotropic with a refractive index difference between n_1 and n3 around 0.8 which is higher than DAST (0.5) suggesting the possibility of phase matching over a wide range of frequencies (see S1-S3 for imaginary part of refractive index)[9]. The accuracy of the refractive index is found to be 0.00086 at 400 eV and 4 x 4 x 1 ***k*** point mesh (see supporting information S4 and S5).

Dielectric permittivity measurements were carried out on the sample which was silver coated and then placed inside a dielectric cell. The capacitance measurements were done for temperature at 55°C, 75 °C, 95 °C and 115 °C in the frequency range 50 Hz to 5 MHz. Figure 7d shows the plot of dielectric constant ε´ as a function of frequency. The dielectric constant varies between 10 and 12 at different temperatures and is almost double that of DAST; this may due to the reason that pelletized powder of DSSS was used instead of single crystals[9]. The important optical properties determined experimentally are found to be an order of two times more than that of DAST crystal which could due to the different anion. If the difference is due the anion then the simulated property should different from that of DAST but it is identical to it, Therefore, the difference of a factor two between the simulated and the measured values could be attributed to some unknown part of the experimental conditions.

Nonlinear Optical Properties

The chromophore's non-centrosymmetric alignment is a prerequisite for SHG and electro-optical modulation. In the case of DSSS crystal it has been observed that the planar stilbazolium chromophores are at an angle of 22° with respect to the a-axis of the crystal (Fig. 8). This alignment in the DSSS crystal is in between that of the commercialized crystals; the DAST crystal with 20° and the DSTMS with 23°, which suggests that extremely large electro-optic and nonlinear coefficients can be expected [9,10]. The second harmonic generation test was done with a DSSS sample (highly supersaturated) using the Kurtz and Perry technique[28].

For a laser input pulse of 0.68 J, the SHG signal (532 nm) of 14 mV and 1820 mV were obtained for Urea and DSSS (particle size of 90 to 100μm) samples respectively. As the particle size decreases (50 to 70 μm and 70 to 90 μm) the SHG efficiency decreases (1540 and 1680 mV) confirming the existence of phase matching property of DSSS. The observed experimental data confirmed a SHG efficiency of DSSS of nearly 130 times that of standard urea (90 to 100μm). DAST crystal is perhaps one of the most widely studied materials for its NLO properties. The data on its second harmonic efficiency, the effective nonlinear optical

coefficient, the phase matching possibilities and the electro-optic co-efficient are discussed and reviewed by many researchers[9, 14]. In case of DAST, a SHG efficiency of nearly 141 times that of standard urea was observed[29]. In the previously reported work on DSSS, the SHG efficiency was found to be nearly equal to that of DAST[18]. It is evident that the SHG efficiency of DSSS is almost same as that of DAST and the small difference is due to the fact that the cations are aligned an extra 1^{o} more with respect to the a-axis compared to DAST[9].

Conclusion

Understanding the growth dynamics of the crystal is the key leading to the fabrication of device. The present investigation provides the growth aspects of DSSS crystal and to control its morphology by varying the supersaturation. The optical properties are investigated and reported. The improvement in the size and the ability to control shape of the crystal assumes much significance as the material is environmentally stable than DAST and at the same time equally efficient.

Acknowledgements

The authors would like to thank Mr. I. A. Andres Munoz, Department of Physics, Faculty of Physical and Mathematical Sciences, University of Chile, for providing powder XRD analysis.

References

1 K. Ajito and Y. Ueno, *IEEE Transactions on Terahertz Science and Technology*, 2011, **1**, 293.
2 M.Tonouchi, *Nature Photon*., 2007, **1**, 97.
3 D. Mittleman, *Sensing with Terahertz Radiation*, 2003, New York: Springer-Verlag.
4 H. Harde, R. A. Cheville, and D. Grischkowsky, *J. Phys. Chem. A*, 1997, **101**, 3646.
5 H. J. Song and T. Nagatsuma*, IEEE Transactions on Terahertz Science and Technology*, 2011, **1**, 256.
6 G. Chattopadhyay, *IEEE Transactions on Terahertz Science and Technology*, 2011, **1**, 33.
7 B. Ferguson and X. C. Zhang, *Nature Mater.*, 2002, **1**, 26.
8 X. C. Zhang, X. F. Ma, Y. Jin, T. M. Lu, E. P. Boden, P. D. Phelps, K. R. Stewart and C. P. Yakymyshyn, *Appl. Phys. Lett*., 1992, **26**, 3080.
9 M. Jazbinsek, L. Mutter and P. Gunter, *IEEE J. Sel. Top. Quant. Electron*., 2008, **5**, 1298
10 S. R. Marder, J. W. Perry and W. P. Schaefer, *Science*, 1989, **245**, 626.
11 H. Adachi, Y. Takahashi, J. Yabuzaki, Y. Mori and T. Sasaki, *J. Cryst. Growth,* 1999, **198-199**, 568.
12 R. Jerald Vijay, N. Melikechi, T. Rajesh Kumar, J. G. M. Jesudurai and P. Sagayaraj, *J. Cryst. Growth*, 2010, **312**, 420.
13 I. Katayama, R. Akai, M. Bito, H. Shimosato, K. Miyamoto, H. Ito, and M. Ashida, *Appl. Phys. Lett.*, 2010, **97**, 021105.
14 M. Stillhart, A. Schneider and P. Gunter, *J. Opt. Soc. Am. B*., 2008, **25**, 1914.
15 Z. Yang, S. Aravazhi, A. Schneider, P. Seiler, M. Jazbinsek and P. Gunter, *Adv. Funct. Mater*., 2005, **15**,1072.
16 Z. Yang, L. Mutter, M. Stillhart, B. Ruiz, S. Aravazhi, M. Jazbinsek, A. Schneider, V. Gramlich and P. Gunter, *Adv. Funct. Mater*., 2007, **13**, 2018.
17 Z. Yang, M. Jazbinsek, B. Ruiz, S. Aravazhi, V. Gramlich and P. Gunter, *Chem. Mater*., 2007, **14**, 3512.
18 J. Ogawa, S. Okada, Z. Glavcheva and H. Nakanishi *J. Cryst. Growth*, 2008, **310**, 836.
19 R. Jerald Vijay, N. Melikechi, Tina Thomas, R. Gunaseelan, M. Antony Arockiaraj, P. Sagayaraj, *J. Cryst. Growth*, 2012, **338**, 170.
20 Z. Yang, L. Mutter, M. Stillhart, B. Ruiz, S. Aravazhi, M. Jazbinsek, A. Schneider, V. Gramlich, and P. Günter*, Adv. Funct. Mater., 2007, **17**, 2018.*
21 R. Jerald Vijay, N. Melikechi, Tina Thomas, R. Gunaseelan, M. Antony Arockiaraj and P. Sagayaraj, *Mater. Chem. Phys*., 2012, **132**, 610.
22 M. A. Lovette, A. R. Browning, D. W. Griffin, J. P. Sizemore, R. C. Snyder, M. F. Doherty, *Ind. Eng. Chem. Res.,* 2008, **47**, 9812.
23 Ivan V Markov, *Crystal growth for beginners; Fundamentals of Nucleation, Crystal Growth and Epitaxy*, World Scientific, 2003.
24 Y. Li, J. Zhang, G. Zhang, L. Wu, P. Fu and Y. Wu, *J. Cryst. Growth*, 2011, **327**, 127.
25 M. A. Lovette and M. F. Doherty, *Cryst. Growth Des*., 2013, **13**, 3341.
26 H. Mizuno, I. Ohnishi, H. Yanagi, F. Sasaki and S. Hotta, *Adv. Mater.,* 2012, **24**, 2404.
27 S. K. Loyalka and C. A. Riggs. Applied Spectroscopy, 1995, **49**, 1107.
28 S.K. Kurtz and T.T. Perry, *J. Appl. Phys*., 1968, **39**, 3798.
29 K. Jagannathan, S. Kalainathan, T. Guanasekaran, N. Vijayan and G. Bhagavannarayana, *Cryst. Growth Des*., 2007, **7**, 859.

Electronic Supplementary Information (ESI) available: Plot of convergence test, real and imaginary part of refractive index of 100, 010 and 001 polarizations. See DOI: 10.1039/b000000x/

Figure Captions

Fig. 1 Photographs of DSSS crystals grown by (a) SMN-SE method,

Fig. 2 Photographs of DSSS crystals grown by ISE method at (a) higher supersaturation, (b) medium supersaturation, (c) lower supersaturation and (d,e) greenish appearance of the same crystals under reflection.

Fig. 3 Powder XRD pattern of DSSS crystals grown by ISE method at (a) higher supersaturation, (b) lower supersaturation and (c) as synthesized DSSS powder.

Fig. 4 Simulated crystal morphology of DSSS single crystal using materials studio software.

Fig. 5 Micrographs of DSSS crystals grown by ISE method (a,b) at high supersaturation, (c, d, e,) at medium supersaturation with stacked c-plates, and (f) at lower supersaturation with perfect single crystal.

Fig. 6 Influence of convection on the growth of DSSS crystals in a petri dish and a beaker.

Fig. 7 (a) Diffuse reflectance spectrum, (b) absorption coefficient calculated from reflectance (c) refractive index 100, 010 and 001 polarizations simulated using materials studio software and (d) Measured dielectric constant.

Fig. 8 The angle between polar axis and the crystallographic a-axis.

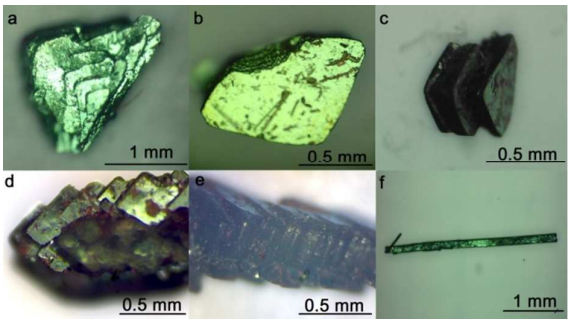

Different morphologies of DSSS crystals are developed by controlling the supersaturation of the solution and the optical properties are investigated.

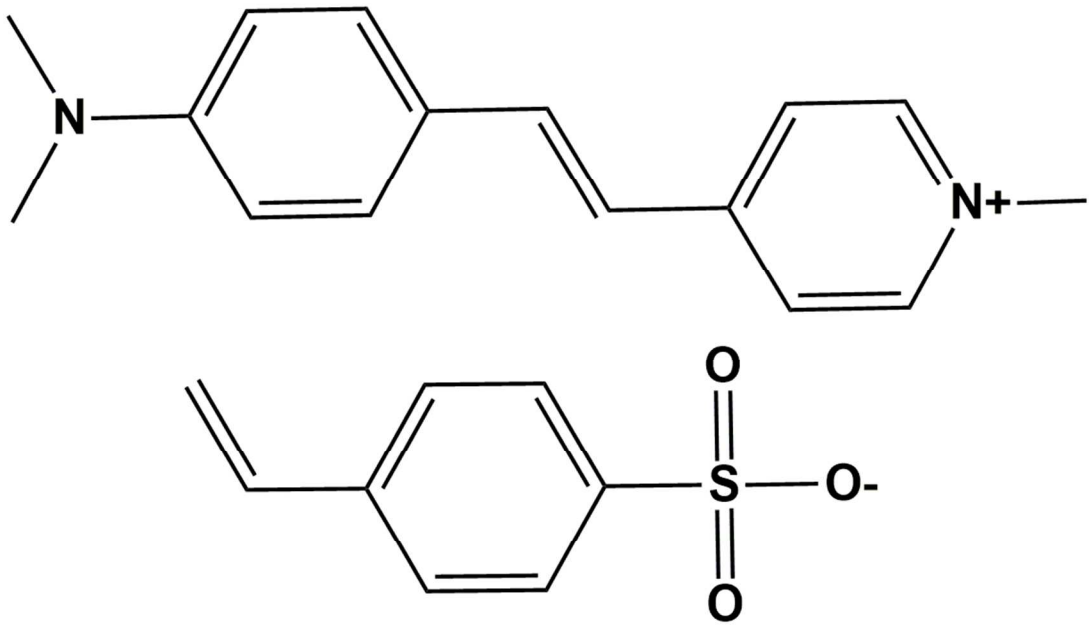

Fig. 1 Chemical structure of DSSS

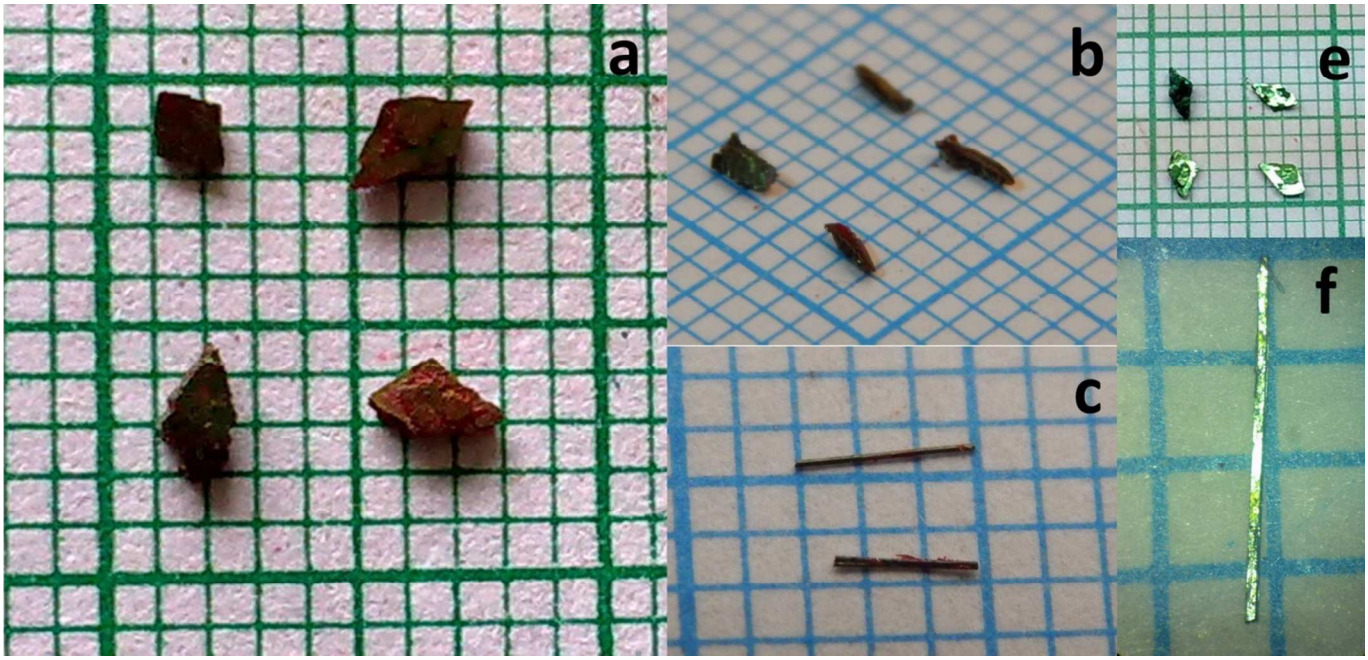

Fig. 2 Photographs of DSSS crystals grown by (a) SMN-SE method, (b) ISE method at higher supersaturation, (c) ISE method at lower supersaturation and (d,e) greenish appearance of the same crystals under reflection.

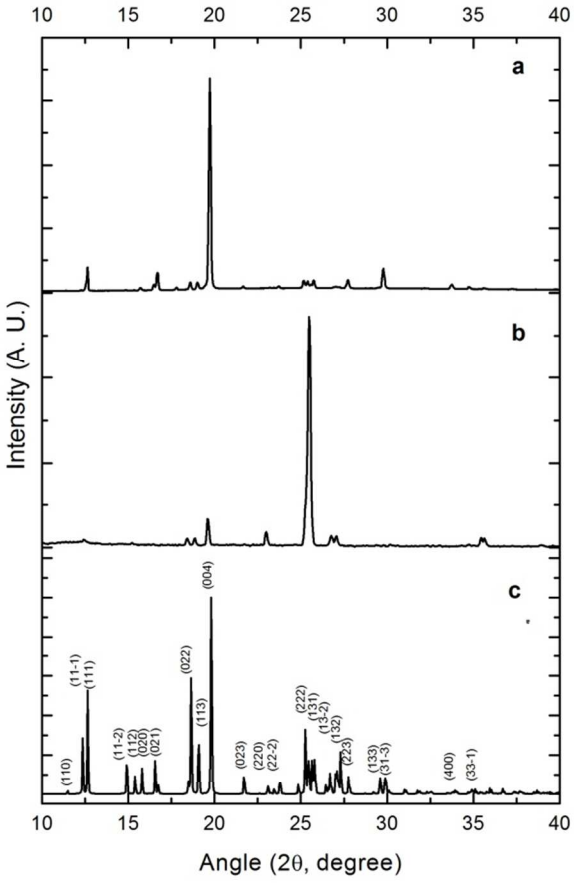

Fig. 3 Powder XRD pattern of DSSS crystals grown by ISE method at (a) higher supersaturation, (b) lower supersaturation and (c) as synthesized DSSS powder.

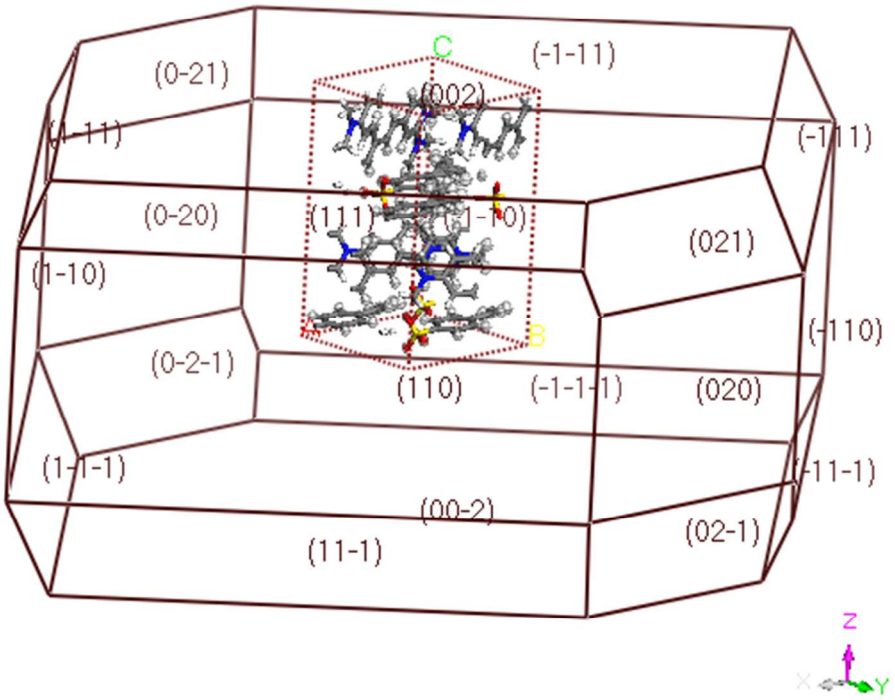

Fig. 4 Simulated crystal morphology of DSSS single crystal using materials studio software.

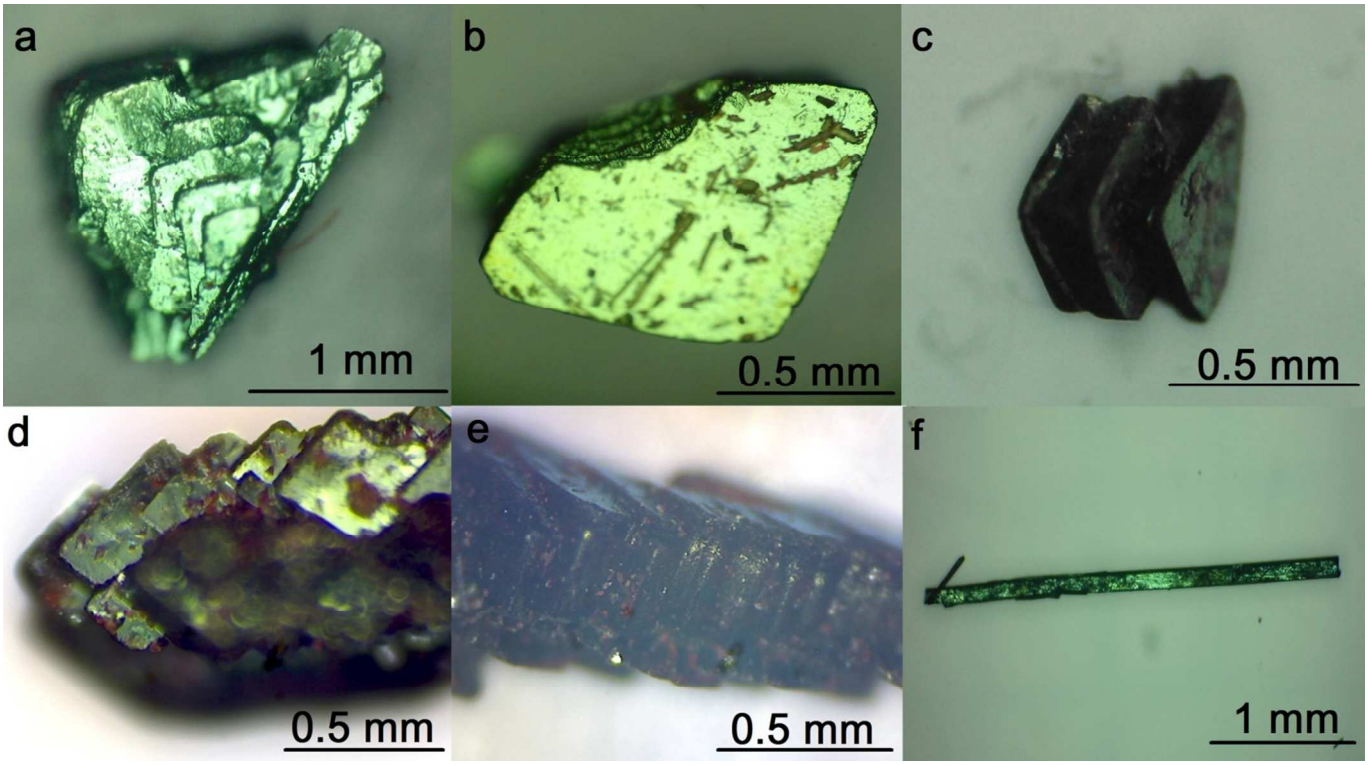

Fig. 5 Micrographs of DSSS crystals grown by ISE method (a,b) at high supersaturation, (c, d, e,) at medium supersaturation with stacked c-plates, and (f) at lower supersaturation with perfect single crystal.

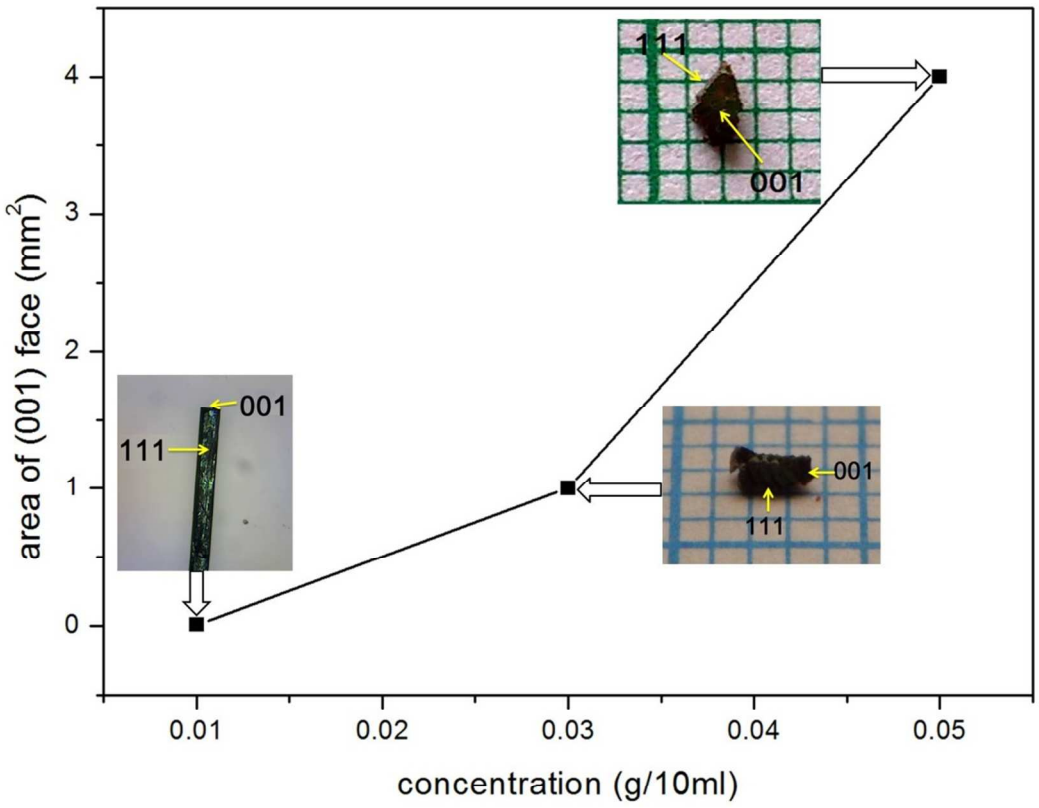

Fig. 6 Influence of supersaturation on the morphology of DSSS crystals.

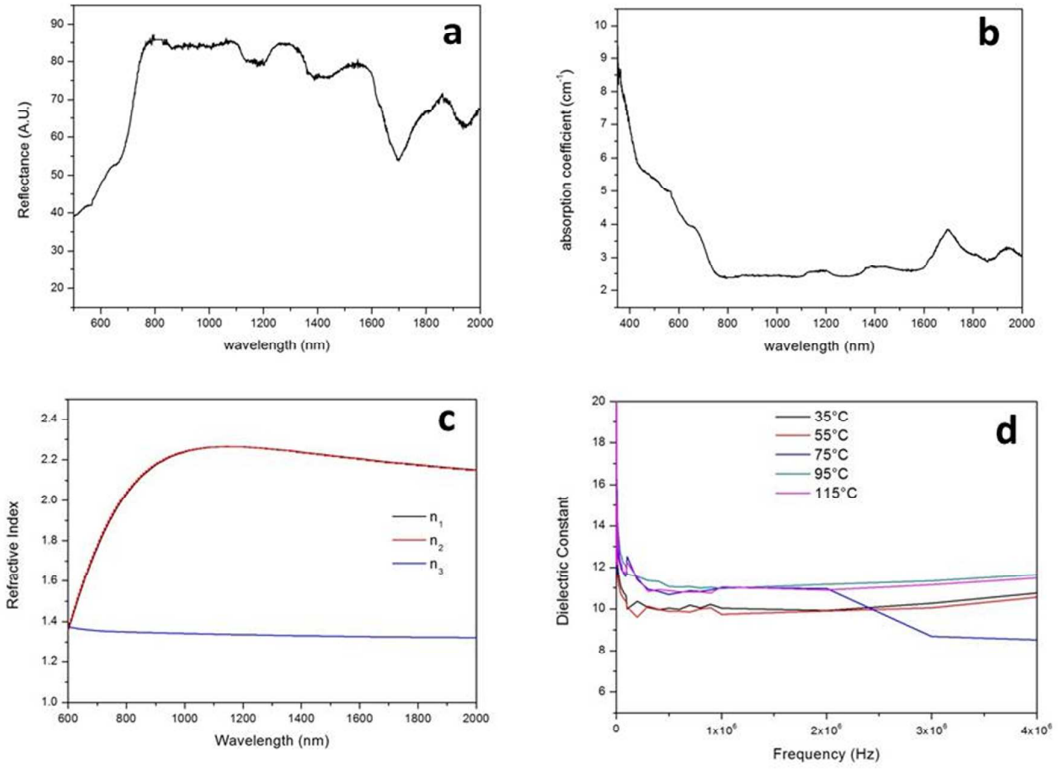

Fig. 7 (a) Diffuse reflectance spectrum, (b) absorption coefficient calculated from reflectance (c) refractive index along 100, 010 and 001 polarizations simulated using materials studio software and (d) Measured dielectric constant.

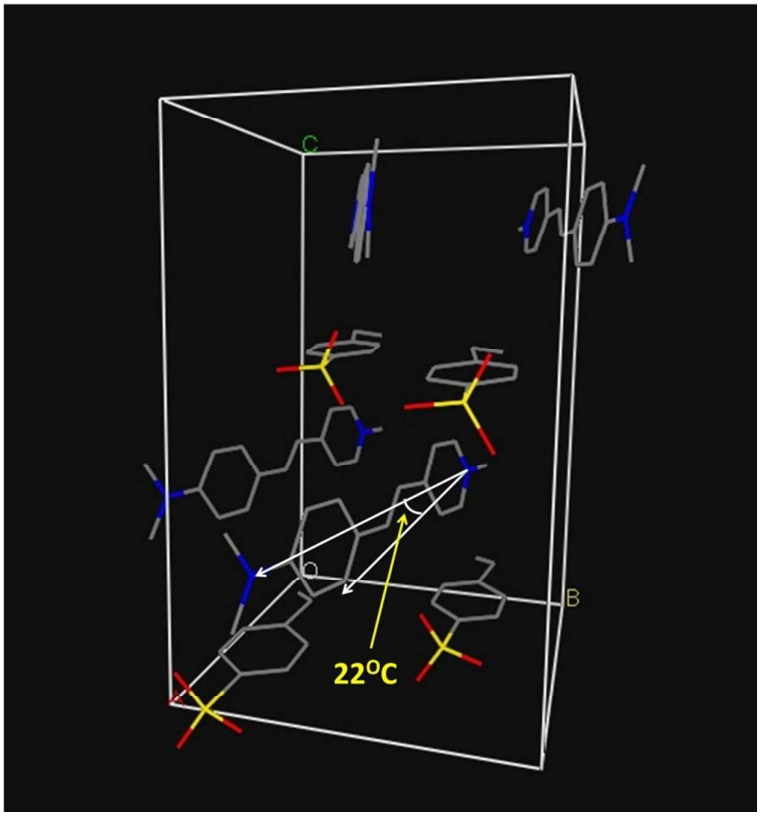

Fig. 8 The angle between polar axis and the crystallographic a-axis.

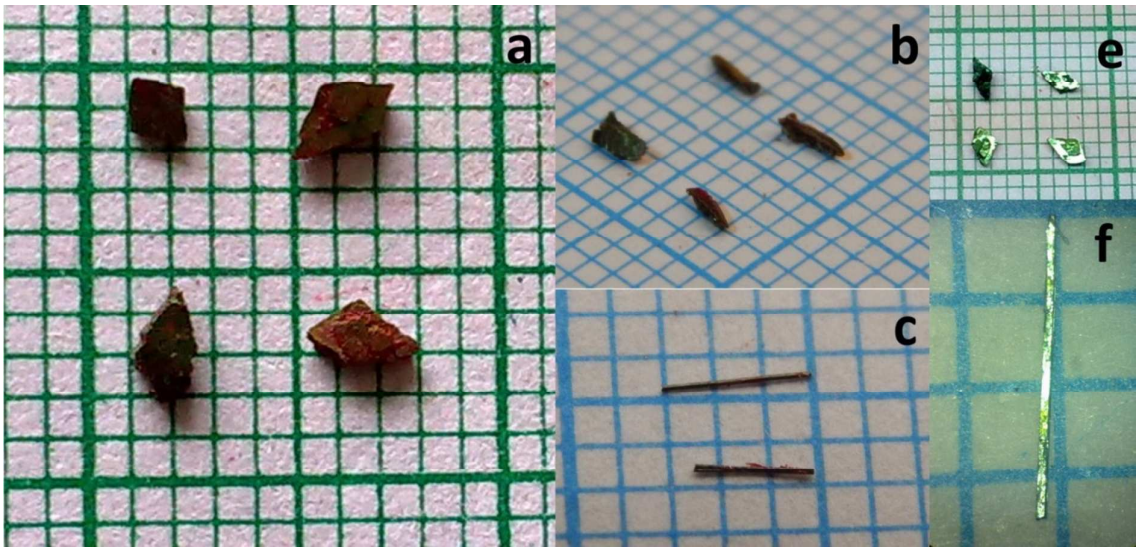

The morphology of the DSSS crystal has been modified from bulk parallelepiped to elongated cuboid shape by changing the supersaturation from high to low respectively. The reproducibility of growing DSSS into a noncentrosymmetric structure in presence of water is further justified by isothermal evaporation method. The growth dynamics and defect mechanisms in mixed solvent system are discussed in detail. Linear and nonlinear optical properties are investigated and reported.